6TH TOPICAL MEETING ON OPTICAL FIBER COMMUNICATION

28 FEBRUARY—2 MARCH 1983

SIXTH TOPICAL MEETING
ON
OPTICAL FIBER COMMUNICATION
28 FEBRUARY–2 MARCH 1983
OSA/IEEE
NEW ORLEANS

Digest of Technical Papers

IEEE catalog number 83CH1850-7

Library of Congress number 82-62850

Printed in the U.S.A.

FOREWORD

The Optical Fiber Communication Conference (OFC) is the major North American conference on the research, technology and application of optical fibers. This year's conference is the sixth in the series that began in Williamsburg, Va. in 1975. Because of the increasing importance of this technology, beginning with the 1982 OFC meeting these conferences will be held annually. OFC is also part of the series of major international conferences that provide worldwide forums for the dissemination of information on the most recent advances in optical guided wave research and development. Every second year the regional conferences in North and South America, Europe and Africa, and the Far East combine to form, in addition to their regular annual meetings, the International Conference on Integrated Optics and Optical Fiber Communications (IOOC) the next of which will be held in Tokyo, Japan, 27–30 June 1983. Additionally, topical meetings on integrated and guided wave optics are sponsored by the Optical Society of America and the Institute of Electrical and Electronics Engineers to discuss work in planar waveguides, semiconductor light sources, and integrated optoelectronics. Beginning in 1984, OFC will alternately meet on the East Coast (New Orleans, 1984) and the West Coast (San Diego, 1985). It is planned that the Conference on Lasers and Electro-Optics (CLEO) will have the opposite alternation to continue to bring the latest advances in both related topic areas to the widest possible audience.

The activity in optical fiber technology is approximately doubling every year, giving OFC a broad mission to accomplish. At one end of the spectrum it must provide the most up-to-the-minute view of technical advances. At the other extreme it must also provide the mechanism for giving new people and organizations the overviews necessary to enter this fast-moving field. The 1983 conference was structured with this in mind. Beginning with an overview, "U.S. Science and Technology—What's Right, What's Wrong, What's Needed" by keynote speaker S. J. Buchsbaum of Bell Laboratories and chairman of the White House Council on Science and Technology, a discussion follows of "Optical Fiber Research—Present and Future" by S. E. Miller of Bell Laboratories and C. Kao of ITT, two of the pioneers in this technology, that will provide review for veterans as well as neophytes in the field. To further help new entrants into the technology a series of nine tutorials covering all aspects from individual components to systems will be presented by some of the leaders in each area. An expanded set of some 30 invited and solicited papers will provide a coherent overview of key aspects of the technology. Last but certainly not least an expanded set of contributed papers presented in three parallel sessions will highlight the latest going on in the field. For the first time a poster session is scheduled, in which papers of more complexity than normal oral presentations will be given. The wide range of topics and multiple levels of presentation should provide conference attendees the information necessary to make it well worth their time. Finally the conference will close with a first-time award ceremony that will recognize and encourage excellence in all facets of fiber research and development. Awards will be presented for the most significant papers at OFC 83 in each of the following categories: fibers and cable, active and passive components, systems and subsystems, and the best presented poster paper. In addition, certificates of commendation will be presented to the instructors who were selected to participate in the tutorial program.

The OFC 83 Program Committee wishes to extend its thanks to scientists and engineers whose contributed works have made this conference possible. The accepted papers illustrate the technical progress that is being achieved in the many laboratories and companies around the world engaged in optical guided wave technology. This continuing series of optical fiber communication meetings is intended to follow and report future developments in optical guided wave technology and to enhance the exchange of technical information in an international forum.

We would also like to express our thanks to Jarus Quinn of the Optical Society of America for the superb job of overseeing the myriad details of this conference. Jarus was most ably assisted by Barbara Hicks, meetings director for the Optical Society of America, and her marvelous staff who are responsible for planning and managing the logistics of this and many other conferences. Special thanks also to Mary Dean VanLandingham for her expert management of the exhibits and to the 60-plus exhibitors which are such a vital part of the information presented at any conference.

We look forward to this and succeeding conferences in which a continued and stimulating interchange of information occurs that in the final analysis is so important to the technical and commercial growth of optical fiber technology.

Sixth Topical Meeting on
OPTICAL FIBER COMMUNICATION

TECHNICAL PROGRAM COMMITTEE

General Chairmen

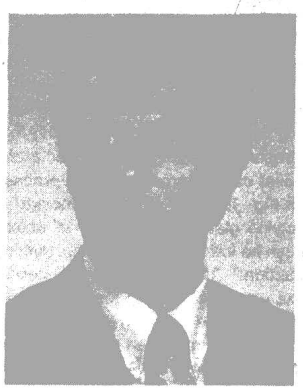

Donald B. Keck
Corning Glass Works
Corning, NY

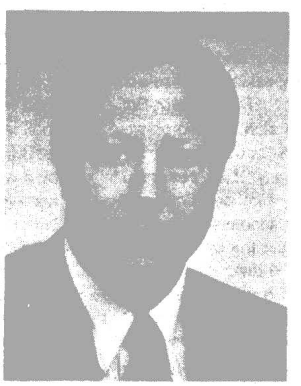

Douglas A. Pinnow
Times Fiber
Communications, Inc.
Wallingford, CT

Program Chairmen

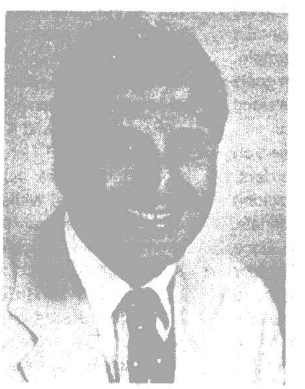

Melvin I. Cohen
Bell Laboratories
Whippany, NJ

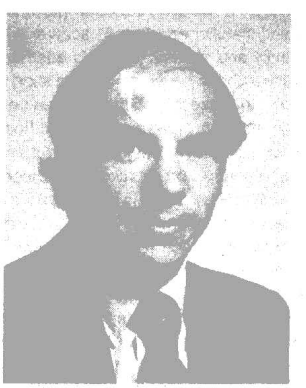

Stewart Personick
TRW Technology
Research Center
El Segundo, CA

Monday MORNING
28 February 1983 MA
BALLROOM E

8.45 AM **Introductory Remarks**

Donald B. Keck, Presider

MA1 U.S. science and technology: what's right, what's wrong, what's needed

SOLOMON J. BUCHSBAUM, Bell Laboratories, Holmdel, N.J. 07733.

Some key issues relating to U.S. science and technology are discussed with special emphasis on the field of communications: support of research and development by government and industry; education; the impact of international competition; regulation and government–industry relations. **(Keynote paper, 60 min)**

Monday MORNING
28 February 1983 MB
BALLROOM E

9:45 AM **Plenary Session**

S. Personick, Presider

MB1 Optical fiber research present and future: telemetry, sensing, and government applications

CHARLES KAO, ITT-ATC, 1 Research Dr., Shelton, Conn. 06484.

Key optical fiber components are being more fully characterized through research efforts. As a result, system product specifications have been firmed up for a range of applications. Much of the current research is toward ensuring that essential and related performance parameters are achieved simultaneously and repeatedly. Essentially, pertinent process parameters are being studied so that appropriate control can be implemented. A nondielectric high-strength small-size fiber cable for wide temperature operation is an example which illustrates the various performance parameters to be achieved simultaneously. A receiver with specific sensitivity and dynamic range is another example. The research work toward meeting short term goals is mainly in these directions and can be illustrated through some targeted system specifications.

Recognizing the design limits, future research efforts are directed at removing these barriers. Thus radiation hardness is being tackled by looking at material systems other than SiO_2-based materials. Fiber durability is receiving continued attention, since it is only marginally adequate for a significantly larger area of applications. Single-mode waveguides are at the base of coherent transmission. Their significances in sensors and signal processing applications are under intensive investigation. Associated with this, optoelectronic techniques realized in ferroelectric and semiconductor integrated circuit forms are developing. This would significantly increase signal processing speed and power and more significantly allow the high-speed signals to be coupled to the transmission medium as well as the terminal electronics. Most of this research takes into account the coherence or lack of coherence of the optical wave. **(Plenary paper, 30 min)**

MB2 Optical fiber telecommunications research

S. E. MILLER, Bell Laboratories, Crawford Hill Laboratory, Holmdel, N.J. 07733.

Research on optical fiber telecommunication systems and components continues in parallel with manufacture and installation of intercity, metropolitan area, and local feeder-link systems. More sophisticated and higher-performance lasers, fibers, and multiplexers will result. Speculative work on materials and coherent optical systems is supported. **(Plenary paper, 30 min)**

Monday MORNING
28 February 1983 MC
BALLROOM E

11.15 AM **Nonoxide Fiber Materials**

G. Tangonan, Presider

MC1 Infrared transmitting fluoride glasses: materials development

MARTIN G. DREXHAGE, Rome Air Development Center, Solid State Sciences Division, Hanscom AFB, Mass. 01731.

Heavy metal fluoride glasses are a recently discovered[1] class of nonoxide vitreous material whose structure, chemistry, and, most important, mid-IR optical behavior are very different from those of silicate glasses. Their compositional flexibility yields glasses with a broad (and controllable) range of optical transmission, refractive index, and dispersion, making them candidates for 2–5-μm waveguides and optical components.[2] Significant amounts of transition metal and rare earth fluorides may also be incorporated within the glass matrix, yielding materials with the potential for unusual magnetic, magnetooptic, or lasing behavior. Demonstration of the suitability of heavy metal fluoride glasses for these and other applications involves preparation and characterization of high-quality bulk glass specimens. Progress and problems in these areas are reviewed, with emphasis on melting and fabrication techniques, viscosity and crystallization phenomena, and the role of additives to enhance glass stability while preserving high optical transparency.

Among the most extensively studied heavy metal fluorides are the fluorozirconate and fluorohafnate glasses; representative compositions and selected properties are shown in Fig. 1. For stability, GdF_3, PbF_2, LiF, NaF, and KF may also be incorporated. Glass transition T_g and crystallization temperatures T_x are much lower than those typically observed in silicate glasses, while expansion coefficients are considerably elevated. In transmission measurements on 1-cm thick samples, the onset of the IR absorption edge occurs at ~6 μm.

A second family of vitreous fluorides is the BaF_2/ThF_4 glasses, examples of which are indicated in Fig. 2. Transmission in these materials extends to 8 μm; replacement of YbF_3 by LuF_3 eliminates a strong absorption band at 1.0 μm, and small additions of GdF_3 and NaF enhance glass stability.

The absorption coefficients in the 6–10-μm region, derived from transmission measurements on polished plates of some heavy metal fluoride glasses, are compared in Fig. 3; these trends are expected to continue at shorter wavelengths. The absorption coefficient is lowered when ZrF_4 is replaced by HfF_4; those of the BaF_2/ThF_4 glasses are observed to be an order of magnitude lower still. Light scattering measurements in properly prepared fluoride glasses show a λ^{-4} behavior with a magnitude approaching that of fused SiO_2. BaF_2/ThF_4 glasses thus present an interesting alternative to fluorozirconate-type materials, as their absorption loss minimum should occur at somewhat longer mid-IR wavelengths. **(Invited paper, 13 min)**

1. M. Poulain, M. Poulain, J. Lucas, and P. Brun, Mater. Res. Bull. 10, 243 (1975).
2. M. Drexhage, O. El-Bayoumi, and C. T. Moynihan, Proc. Soc. Photo-Opt. Instrum. Eng. 320 (1982).

MC2 Infrared transmitting fluoride glasses: fibers

GEORGE H. SIGEL, JR., and D. C. TRAN, U.S. Naval Research Laboratory, Washington, D.C. 20375.

Recently zirconium fluoride-based glasses have emerged as leading candidates for ultralow-loss fiber applications in the mid-IR region because of their superior glass-forming ability relative to many other halide glasses. However, compared with the silica-based glass systems, the fluorozirconate glasses generally exhibit an extremely narrow working range of only ~75°C and a much larger change in shear viscosity with respect to small temperature fluctuations in the fiber drawing regime.[1] These departures from the oxide glass behavior can result in severe devitrification or frequent fiber rupture during the drawing process. To suppress the crystallization tendency and the high activation energy for viscous flow of the zirconium fluoride glasses, it is necessary to incorporate modifiers such as AlF_3, LiF, NaF, PbF_2, and SbF_3. Multicomponent zirconium fluoride-based optical fiber glass systems currently under extensive investigation include ZrF_4–BaF_2–LaF_3–AlF_3–LiF–PbF_2,[1] ZrF_4–BaF_2–GdF_3–AlF_3–SbF_3,[2] ZrF_4–BaF_2–LaF_3–AlF_3–NaF,[3] and ZrF_4–HfF_4–BaF_2–ThF_4–LaF_3–AlF_3–LiF–NaF.[4] This paper will provide an overview of the present status of fiber and preform preparation for these materials.

To date, fluoride glass fiber fabrication using the vapor phase deposition technique has not been initiated due to the very high vapor pressure associated with the fluoride glass components. Instead fluoride glass fibers have been successfully prepared from bulk glasses using both the preform casting technique and the crucible approach. The first fluoride glass preform, reported by Mitachi *et al.*,[5] was prepared by shrinking a Teflon FEP tubing over a core glass rod. Subsequently Manabe *et al.*[2] reported the fabrication of a zirconium fluoride-based glass-cladded preform by the built-in casting technique which consists of allowing the cladding melt in a mold to flow out and then casting the core melt into the tube thus obtained. Recently Tran *et al.*[6] have prepared fluoride glass-cladded preforms by a rotational casting process. This process, illustrated in Fig. 1, yields a highly concentric and uniform fluoride glass-cladding tube in which the core melt can be introduced by casting, dipping, or vacuum suction. The superimposed step-index profiles of a rotational casting preform measured over a 6-in. interval, as shown in Fig. 2, suggest that a uniform core–clad ratio can be obtained which permits the upscaling to very large preforms. Presently attenuation levels as low as 12 dB/km have been achieved at 2.55 μm utilizing the preform casting technique, ultrahigh-purity fluoride raw materials, and a localized heat zone electrically heated platinum furnace.[2]

The alternate crucible drawing approach offers the potential advantages of a continuous process coupled with a rapid quenching capable of suppressing crystallization in the finished fluoride glass

	ZBLA	HBLA	ZBL	HBL
mol %				
ZrF_4	57	--	62	--
HfF_4	--	57	--	62
BaF_2	36	36	33	33
LaF_3	3	3	5	5
AlF_3	4	4	--	--
Density (gm/cc)	4.61	5.88	4.79	5.78
T_g (°C)	310	312	306	312
T_x (°C)	390	400	380	395
Refractive Index n_D	1.516	1.504	1.523	1.514
Expansion Coefficient ($^oC^{-1}$)	187×10^{-7}	173×10^{-7}	188×10^{-7}	177×10^{-7}

MC1 Fig. 1. Compositions and selected properties of representative fluorozirconate and fluorohafnate glasses.

GLASS	COMPOSITION (mol %) BaF_2	ZnF_2	YbF_3	LuF_3	ThF_4	MF$_n$	T_x-T_g (°C)	T_g (°C)	T_x (°C)	THERMAL EXPAN. ($^oC^{-1}$)
1	19	27	27	---	27	---	63	364	427	
2	19	27	---	27	27	---	76	353	429	151×10^{-7}
3	19	26	---	26	26	6 GdF_3	75	357	432	151×10^{-7}
4	19	26	26	---	26	3 GdF_3	49	359	408	
5	19	26	26	---	26	3 LaF_3	51	358	409	
6	19	26	26	---	26	3 BiF_3	79	354	433	
7	14	27	27	---	27	5 NaF	82	343	425	

MC1 Fig. 2. Compositions and selected properties of representative BaF_2/ThF_4-containing fluoride glasses.

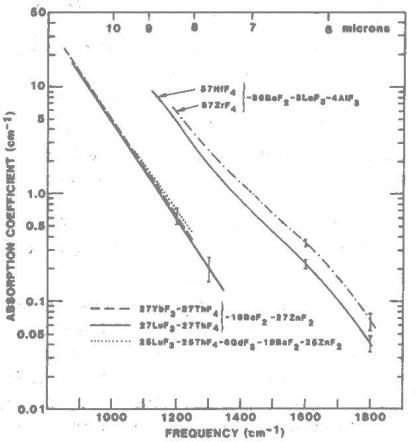

MC1 Fig. 3. Absorption coefficients vs frequency/wavelength for some of the glasses of Figs. 1 and 2.

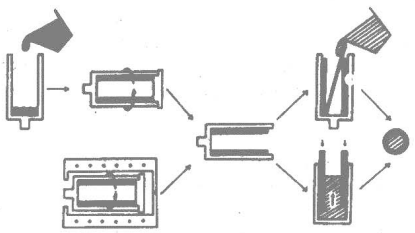

MC2 Fig. 1. Rotational casting process.

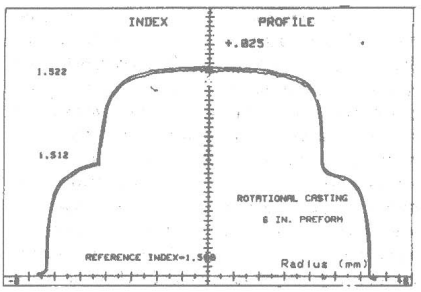

MC2 Fig. 2. Index profiles of a rotational casting preform.

fiber. Tran *et al.* have demonstrated the fabrication of unclad ZrF_4–BaF_3–LaF_3–AlF_3–LiF–PbF_2 fibers in lengths up to 1 km using the single crucible technique.[1] High scattering losses, however, were often observed in these fibers which appear to be associated with crystallization induced by quenching temperatures. Proper draw conditions, such as quenching rates, temperatures, and the nucleation and growth phenomena of the fluoride glasses, associated with the crucible drawing technique, are being investigated and will be reported.

In summary, substantial advances in both preform fabrication and fiber drawing techniques have resulted in rapid reduction of attenuation levels in fluoride glass fibers. This has been achieved by taking into account the unique properties of the glasses relative to oxides and by properly modifying fiber fabrication procedures to accommodate these fluoride characteristics. **(Invited paper, 13 min)**

1. D. C. Tran, R. J. Ginther, and G. H. Sigel, Jr., Mater. Res. Bull. 17, (9) (1982).
2. T. Manabe *et al.*, in Domestic Conference of the Institute of Electronics and Communication Engineering, Japan (Aug. 1982).
3. K. Ohsawa, T. Shibita, K. Nakamura, and M. Kimura, at First International Symposium on Halide and Other Non-Oxide Glasses (Cambridge, 1982), paper 5D.
4. H. Poignant, O. Regreny, and D. Montomet, at First International Symposium on Halide and Other Non-Oxide Glasses (Cambridge, 1982), paper 9D.
5. S. Mitachi, S. Shibata, and T. Manabe, Electron. Lett. 17, 170 (1982).
6. D. C. Tran, C. F. Fisher, and G. H. Sigel, Jr., Electron. Lett. 18, No. 657 (1982).

MC3 Minimization of OH absorption and scattering losses in zirconium fluoride glasses

D. C. TRAN, C. F. FISHER, K. L. LEVIN, and GEORGE H. SIGEL, JR., U.S. Naval Research Laboratory, Washington, D.C. 20375.

The most important criterion in maximizing the IR transparency of fluoride glasses for low-loss optical fiber applications is the elimination of the anionic impurities, mainly OH, which enter the glass during the batching and melting processes.[1] By analogy with the OH absorption coefficient in silica glass fiber, it was estimated that 1-ppm OH would give rise to a 5000-dB/km loss at 2.9 μm[2] in fluoride glass fibers. In addition, particle inclusions, phase separation, and submicron inhomogeneities or crystallization, which result in high scattering losses, must be totally suppressed. Previously the minimum OH absorption loss reported for a fluoride glass fiber was ~1000 dB/km at 2.9 μm[2], and the lowest scattering loss contribution for a fluoride glass rod was estimated to be 65 dB/km at 0.633 μm.[2] In this paper, substantially lower losses have been achieved using reactive atmosphere processing to remove OH and proper melting, refining, and quenching conditions to eliminate scattering imperfections.

Reactive atmosphere processing of zirconium fluoride-based glasses using SF_6, HF, CCl_4, CF_4, and NH_4HF_2 has been conducted. The extent of bulk OH removal determined as a function of reaction time, processing temperature, and gas flow rate has been studied. The effects of impurities, side reaction, and material degradation originating from the reactive atmosphere on the optical transparency of the fluoride glasses will be discussed. In Fig. 1, spectrum *A* shows an intensive absorption band corresponding to an ~78,000-dB/km loss at 3400 cm^{-1} due to surface and bulk OH for a zirconium fluoride-based glass processed under an inert gas atmosphere. The effect of processing the same sample under an SF_6 reactive atmosphere is illustrated in spectrum *B*. The residual OH absorption band in curve *B* remained unchanged with sample thickness suggesting that essentially only surface OH remains after such processing.

The scattering losses in bulk fluorozirconate glasses have also been investigated as a function of melting and refining procedures, quenching rates, and fiber drawing temperatures. The scattering loss was measured using an Ar-ion laser and a He–Ne laser in conjunction with a silicon photodiode detector. The light signal from a small solid angle was detected as a function of scattering angle and wavelength. The measurement system was calibrated using benzene as a standard. Figure 2 illustrates the lowest scattering loss currently achieved for a zirconium fluoride glass, matching that of a high-purity Suprasil I and following a λ^{-4} wavelength dependence characteristic of intrinsic Rayleigh scattering.

In summary, this paper reports advances in two areas essential for the development of high-transparency fluoride glass fibers, namely, OH removal and sharply reduced scattering losses. This has been achieved by utilization of both reactive SF_6 atmosphere processing as well as optimized thermal processing of the bulk glass. **(13 min)**

1. C. F. Fisher, D. C. Tran, and G. H. Sigel, Jr., at Fall Meeting of the American Ceramic Society, Bedford Springs, Pa. (1982).
2. S. Mitachi and T. Miyashita, Electron. Lett. 18, 170 (1982).

MC4 Low-loss plastic optical fibers

TOSHIKUNI KAINO, KANAME JINGUGI, and SHIGEO NARA, NTT Ibaraki Electrical Communication Laboratory, Plastic Moulding Section, Tokai, Naka-gun, Ibaraki 319-11, Japan.

The closed polymerization and fiber drawing method[1] was very effective in lowering the attenuation loss of plastic optical fiber (POF). Using this method, we developed low-loss POFs of PMMA core, which had the lowest attenuation, 55 dB/km, at a 568-nm wavelength as shown in Fig. 1.

The attenuation loss of this POF is composed of intrinsic absorption due to carbon—hydrogen (C—H) vibration and electronic transition, intrinsic Rayleigh scattering, and extrinsic scattering due to imperfections in the waveguide structure α_l as shown in Fig. 1. The structural regularity and the molecular orientation due to the fiber drawing, which are characteristic of POF, have little influence on α_l. The orientational birefringence of $<1 \times 10^{-4}$ does not bring about any loss increase in the POF.

When the POF is used as an optical signal transmission medium, the carrier wavelengths must be closely matched to the peak emission wavelength of the display-grade LED (a cheap optical source). Among display-grade LEDs, GaAlAs, whose emission wavelength is 660 nm, has the highest output level. The attenuation loss of the PMMA core POF at 660 nm is 160 dB/km. The loss at this wavelength is mainly prescribed by the C—H vibrational absorption, as shown in Fig. 1.

To reduce C—H vibrational absorption, conversion of hydrogen in C—H bonds to deuterium (D) is expected.[2] Results using deuterated PMMA [P(MMA-d8)] as a core for optical fibers have been reported by Schleinitz.[3] It has carrier wavelengths at 690 and 790 nm, but the loss of this P(MMA-d8) core POF was 180 dB/km at best.

The P(MMA-d8) core POF with fluorinated alkyl methacrylate copolymer cladding was fabricated by the same method as PMMA core POF. As shown in Fig. 2, this fiber has the lowest attenuation, 20 dB/km, at 650–680-nm wavelengths. By converting H to D, the peak wavelength of higher harmonics of C—D absorption are shifted to the longer wavelength region, 200 nm or more of that of C—H absorption, and the strength of C—D absorption is lowered to about a quarter of those of the same quantum number C—H absorption.

The loss limit of this P(MMA-d8) core POF is estimated to be 10 dB/km, at 680 nm. The value can be realized if the loss from α_l is excluded.

The P(MMA-d8) core POF can give 1300-m length optical signal transmission at −34 dBm up to 10 MHz using the display-grade GaAlAs LED (whose emission power is 1 mW) and a PIN photodiode as the receiver. By changing C—D contents in the POF, transmission lengths will be changed as shown in Fig. 3; 62.5% C—D conversion, which can be fabricated cheaply using P(MMA-d5), will transmit optical signals for ~400 m.[4]

As C—H vibrational absorption becomes negligible, O—H vibrational absorption due to water absorption of the core polymer is detected especially in the near-IR region. Although the effect of O—H absorption in the visible is small, the P(MMA-d8) core POF is adaptable to intrabuilding optical signal transmission with the benefit of its handling and splicing ease using cheap optical sources. **(13 min)**

1. T. Kaino, M. Fujiki, S. Oikawa, and S. Nara, Appl. Opt. 20, 2886 (1981).
2. T. Kaino, M. Fujiki, and S. Nara, Polym. Prepr. Jpn. 30, 544 (1981).
3. H. M. Schleinitz, at International Wire and Cable Symposium (1977), Vol. 25, p. 352.
4. T. Kaino, K. Jinguji, and S. Nara, Appl. Phys. Lett. 41, (8) (1982).

Monday **MORNING**
28 February 1983 **MD**
BALLROOM H

11:15 AM Undersea systems

Larry U. Dworkin, Presider

MD1 Worldwide status of undersea lightwave system development

I. W. STANLEY, British Telecom Research Laboratories, Martlesham Heath, Ipswich, Suffolk IP5 7RE, U.K.

Submarine system technology is now undergoing a more revolutionary change than at any time since the first voice-circuit cables entered service in 1956. A simultaneous evolution from analog to digital techniques and from copper to optical fiber for the transmission medium poses a unique combination of challenges to be solved before the first systems are due to enter service in the mid-1980s. The purpose of this talk is to present a summary of announced trials and briefly review the current state of development of the technologies likely to be used in first-generation systems with particular reference to optical techniques. Laser types and reliability will be summarized together with the performance of current fiber designs. The relative characteristics of avalanche photodiodes and PIN diode detectors will also be considered.

Avenues of development that are aimed at extending repeater spacings in monomode systems will also be outlined, including recent coherent optical system experiments based on homodyne and heterodyne techniques at 1.5 μm. The relative merits and characteristics of monomode fibers designed to have their loss and dispersion performance

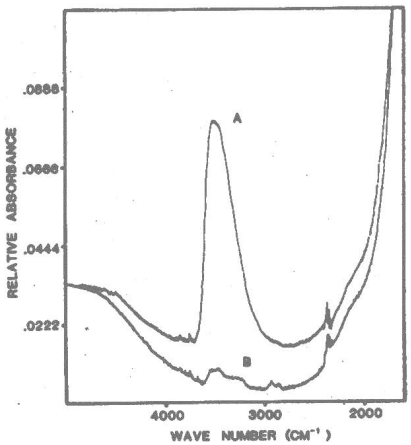

MC3 Fig. 1. OH absorption of a 51.53 ZrF_4–20.47 BaF_2–5.27 LaF_3–3.24 AlF_3–19.49 LiF glass before and after an SF_6 reactive atmosphere processing.

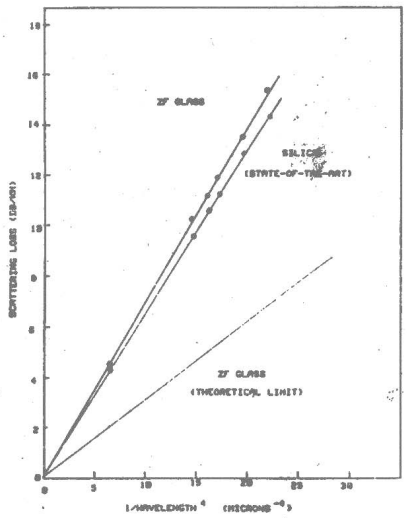

MC3 Fig. 2. Rayleigh scattering of a 51.53 ZrF_4–20.47 BaF_2–5.27 LaF_3–3.24 AlF_3–19.49 LiF glass.

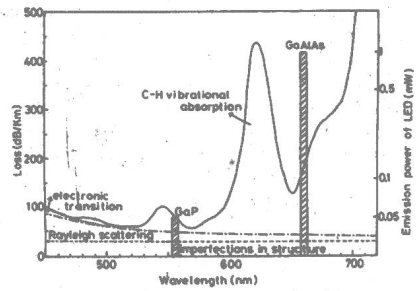

MC4 Fig. 1. Loss spectrum and loss factors of PMMA core POF.

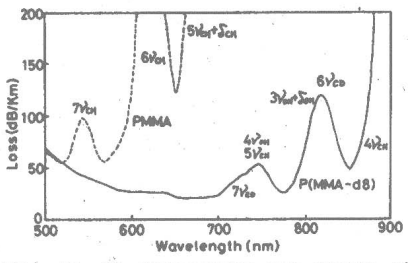

MC4 Fig. 2. Transmission loss spectra of P(MMA-d8) core POF.

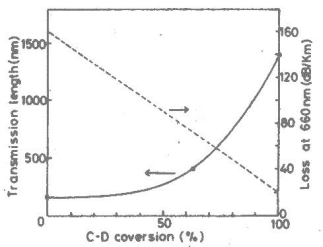

MC4 Fig. 3. Relationship between C—D conversion and transmission length.

at 1.3 and 1.5 μm optimized in various ways will be given. A summary of the factors likely to limit system performance based on the further development of present transmitter, fiber, and receiver technologies will also be presented.

(Invited paper, 25 min)

MD2 Deep-sea trial of an undersea lightwave system

P. K. RUNGE, Bell Laboratories, Holmdel, N.J. 07733.

In early Sept. 1982, the major components of the SL Undersea Lightwave system were tested in what is believed to be the first deep-sea trial of any lightwave system. An 18-km lightwave cable plus a repeater were laid in over 5.5-km deep water in the Atlantic Ocean ~660 nmi ENE from Bermuda. Transmission was monitored through twelve single-mode fibers and two submersed regenerators during laying, holding, and recovery operations. The presentation will discuss details of the operations and the measurements. **(Invited paper, 25 min)**

Monday **MORNING**

28 February 1983 **ME**

BALLROOM F

11:15 AM **Minitutorial: Fiber Optics Theory and Overview**

Paul D. Lazay, Bell Laboratories

An overview of light-wave systems will be presented covering the fundamentals of light propagation in optical fibers, devices required for a complete light-guide system, and the general areas of application of such systems. Information will be presented describing the operation of both multimode and single-mode light-wave systems.

Paul D. Lazay received the B.S. degree in physics from Trinity College in 1961 and the Ph.D. degree in physics from MIT in 1968. He joined Bell Laboratories in 1969 and has been involved in a wide range of research on physics and optical phenomena in materials. Until October of 1982, Lazay was supervisor of the Optical Measurements and Process Control Group at Bell Laboratories, Murray Hill, New Jersey. He is currently with ITT Electro-Optics Division in Roanoke, Virginia. Lazay is a member of the Optical Society of America and the American Physical Society.

(Minitutorial, 60 min)

NOTES

Monday **AFTERNOON**

28 February 1983 **MF**

BALLROOM E

2:00 PM **Single-Mode Fiber Design**

A. Sarkar, Presider

MF1 Single-mode fiber design

DONALD B. KECK and V. A. BHAGAVATULA, Corning Glass Works, Research & Development Division, Corning, N.Y. 14831.

With the increasing importance of monomode fibers, considerable thought has been devoted to design optimization. For telecommunications the technical goal of this work has been the simultaneous minimization of all forms of loss and dispersion over the widest possible wavelength region and with the broadest tolerance on key fiber parameters.

Physically the quantity controlling performance and, therefore, design is the radial mode power distribution usually measured by the mode spot size ω and its variation with wavelength. To minimize intrinsic scattering and interconnection loss, the power should be spread over a large radial region. A large spot size is also beneficial, since power distributed over regions with differing index and dispersion can significantly alter the total waveguide dispersion. However, microbending and macrobending losses are minimized by designs which restrict the mode field distribution. These physical requirements are in obvious conflict. For the near term, a compromise between these requirements using comparatively simple waveguide structures will likely be employed. More complex structures which may partially overcome these conflicts are being investigated for the future.

The five single-mode designs currently receiving most attention are illustrated in Fig. 1. Quite detailed design studies have been done for both the simple step and depressed cladding designs,[1,2] and both seem capable of handling the immediate applications with little difference in expected performance. While the depressed cladding may have slightly lower intrinsic scattering (~0.04 dB/km) due to a reduction of germanium dopant, macrobending loss in certain situations may be greater. The total dispersion for either is less than ~3 psec/nm km at 1300 nm, sufficiently low for many applications. Both are likely to see widespread use in the coming year.

For the future, an incrementally lower loss can be obtained in the 1500–1600-nm region. However, a reduction of dispersion either by shifting λ_0 or balancing material and waveguide dispersion over a wide region will be necessary. The W-profile structure[3] has been shown to both shift λ_0 and flatten the dispersion.[4,5] However, the attenuation characteristics may not be as favorable, and tolerances are indicated to be severe. An $\alpha \approx 1$ profile fiber has been shown to shift λ_0 to ~1550 nm while still maintaining low intrinsic scattering.[6,7] While interconnection may be incrementally more difficult, the bending properties should be more favorable. Using still more complex segmented profile structures,[8,9] rather flat dispersion and favorable loss characteristics are simultaneously possible.

At the present time it appears technically possible to achieve the broad goal of single-mode design. It should be cautioned, however, that tremendous work is still required to determine the system cost effectiveness of these newer proposals.

(Invited paper, 25 min)

1. V. A. Bhagavatula, D. B. Keck, R. A. Westwig, and P. E. Blaszyk, in *Technical Digest, Topical Meeting on Optical Fiber Communication* (Optical Society of America, Washington, D.C., 1982), paper THCC4.
2. P. D. Lazay and A. D. Pearson, in *Technical Digest, Topical Meeting on Optical Fiber Communication* (Optical Society of America, Washington, D.C., 1982), paper THCC2.
3. S. Kawakami and S. Nishida, IEEE J. Quantum Electron. **QE-10,** 879 (1974).
4. T. Miya, K. Okamoto, Y. Ohmori, and Y. Sasaki, IEEE J. Quantum Electron. **QE-17,** 858 (1981).
5. S. J. Jang, L. G. Cohen, W. L. Mammel, and M. A. Saifi, Bell Syst. Tech. J. **61,** 385 (1982).
6. M. A. Saifi, S. J. Jang, L. G. Cohen, and J. Stone, Opt. Lett. **7,** 43 (1982).
7. B. J. Ainslie, K. J. Beales, D. M. Cooper, C. R. Day, and J. D. Rush, Electron. Lett. **18,** 842 (1982).
8. L. G. Cohen, W. Mammel, and S. J. Jang, Electron. Lett. submitted for publication.
9. V. A. Bhagavatula and P. E. Blaszyk, in *Technical Digest, Topical Meeting on Optical Fiber Communication* (Optical Society of America, Washington D.C., 1983), paper MF5.

MF2 Optimum design of 1.3- and 1.55-μm monomode fibers

C. A. MILLAR, M. H. REEVE, S. HORNUNG, and D. B. PAYNE, British Telecom Research Laboratories, Martlesham Heath, Ipswich, Suffolk IP5 7RE, U.K.

Recent laboratory demonstrations of long-distance large-bandwidth monomode systems have been followed by several successful field-installed links. They have shown that monomode fibers can be placed in cables, pulled into ducts, spliced, and measured in realistic environments. To achieve the performance required by the system's designer, the optical characteristics of the fibers in a real link must be prudently chosen to minimize total transmission loss. We shall consider the fiber design which satisfies this criterion for fibers that are loss-limited at 1.3 and 1.55 μm, that is, in the notation of Ainslie *et al.*,[1] type *B* matched-cladding fibers with zero total dispersion of ~1.3 μm.

The equivalent step-index (ESI) technique has been proposed as a method of describing monomode fibers with irregular profile features and variations, and several measurement methods exist to define the two unique and wavelength-independent parameters a_e and Δn_e, which describe the fiber.[2,3] However, it is clearer to discuss measured rather than derived quantities in the analysis of an optimum fiber design, and we shall use two measurable entities—the exp(−1) radial mode field width at 1.3 μm $w_{1.3}$ and the LP_{11} mode cutoff wavelength λ_{co}—as the fiber specifiers. This does not restrict the application of ESI profiles, since a_e and Δn_e can be inferred from $w_{1.3}$ and λ_{co}. Plotting $w_{1.3}$ against λ_{co} gives a plane of operation where system fibers can be positioned (Fig. 1).

Clearly the fiber must be single mode in operation, placing an upper limit on λ_{co}. If a safe margin is allowed for source wavelength variation λ_m, we find $\lambda_{co} < 1.275$ μm [(*a*) in Fig. 1].

The overall loss of a link of concatenated fibers is governed by (a) cabling loss α_c; (b) fiber loss (in addition to Rayleigh scatter loss) due to (1) dopant level-dependent loss $\alpha_{\Delta n_e}$ and (2) OH loss α_{OH}; (c) splice loss (other than the splicing technique) due to (1) concentricity error α_{conc} and (2) field mismatch $\alpha_{\Delta w}$.

Fibers show a rapid susceptibility to cabling loss as a function of w and V (or λ_{co}).[4] If an upper limit of 0.05 dB/km is an allowable cabling margin, the boundaries of that loss of 1.55 μm (directly from Ref. 4) and 1.3 μm (data of Ref. 4 shifted for same loss) are shown as (*b*) and (*c*) in Fig. 1.

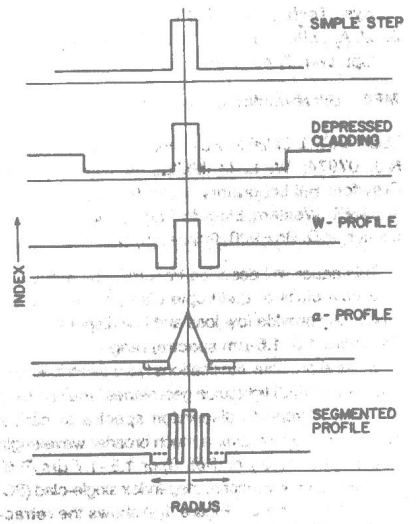

MF1 Fig. 1. Schematic of the single-mode refractive-index profiles under study.

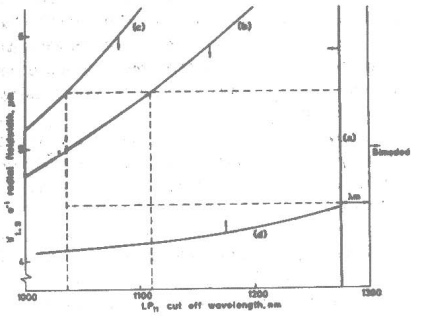

MF2 Fig. 1. Measured fiber parameters.

Fiber losses increase with the Ge-dopant level and OH content. For a given λ_{co} increasing index differences translate to decreasing field widths, so the dopant level-dependent loss places a lower boundary line to $w_{1.3}$. Empirical data from several BT systems and particular cable designs reveal[5] $\alpha_{\Delta n_e} = 0.22 + 56.3\Delta n_e$ dB/km. For a water peak height of 2 dB/km, the OH loss is ~0.05 dB/km at 1.3 μm. In Fig. 1 the $\alpha_{\Delta n_e}$ loss after removal of the α_{OH} loss is shown as boundary line (*d*); 0.5 dB/km is taken as a limit value in this case. A clear triangular zone of operation now appears in Fig. 1, bound by lines (*a*), (*b*), or (*c*) and (*d*).

This zone is further restricted by splicing considerations, which relate to the overall system via the splice interval and the average splice loss. For a given concentricity error, α_{conc} reduces with increasing $w_{1.3}$ so the desire is to operate in the top-right region of the triangle, where unfortunately the area between the cabling losses and the upper cutoff bound is narrowest. It would be best to operate in the widest region of the triangular area (largest tolerance in cutoff) and control the concentricity at the production stage. An operating radial field width of ~5 μm is a good compromise.

For state-of-art splicing techniques and splice intervals of 1.5 km, an acceptable allowance for average splice loss due to field mismatch $\alpha_{\Delta w}$ is 0.05 dB. This can be achieved with a spread in field width of about the 5-μm value of $\pm$0.5 μm. The upper bound of 5.5 μm on $w_{1.3}$ results in two lower bounds of λ_{co} depending on whether a 1.3-μm-only or a 1.3- + 1.55-μm window system is required. For the former $\lambda_{co} > 1.03$ μm, and for the latter $\lambda_{co} > 1.11$ μm. The small difference in the specification for the dual-window fiber implies that the benefits of providing 1.55-μm extendable links can be achieved with only a slight tightening of the fiber specification.

Based on an analysis of the dependence on system loss by the various loss contributors, measured fiber parameters are used to optimize the design of type *B* monomode fiber. For dual-window operation fiber values in the range 5.5 μm $> w_{1.3} >$ 4.5 μm and 1.275 μm $> \lambda_{co} >$ 1.11 μm are found to be optimum. **(13 min)**

1. B. J. Ainslie *et al.*, IEEE J. Quantum Electron. **QE-18**, 514 (1982).
2. F. Alard *et al*, Electron. Lett. **17**, 958 (1981).
3. C. A. Millar, in *Technical Digest, Topical Meeting on Optical Fiber Communication* (Optical Society of America, Washington, D.C., 1982), paper THEE3.
4. S. Hornung and M. H. Reeve, Electron. Lett. **17**, 774 (1981).
5. S. Hornung, to be published.

MF3 Graded-index single-mode fibers with zero dispersion at 1.55 μm

S. J. JANG, M. J. POTASEK, K. D. POHL, and T. L. WATROS, Western Electric Engineering Research Center, P.O. Box 900, Princeton, N.J. 08540.

Recently single-mode fibers with α-index profiles have been analyzed[1,2] and fabricated.[3] These results indicated that very low-loss fibers with larger core diameters than step-index types can be made which also operate with zero dispersion at longer wavelengths than 1.3 μm.

In this paper we disclose the fabrication of a fiber with a triangular-index profile having a zero dispersion near 1.55 μm. The preform was made using the MCVD method in which fifty cladding layers with a refractive index the same as fused silica were deposited followed by six germania-doped core layers. The fibers were drawn in an rf induction zirconia furnace with core diameters of 6.2 and 6.7 μm, each 1 km long.

Losses were measured to be 0.27 dB/km at 1.553 μm, and the minimum loss was 0.26 dB/km at 1.6 μm. Figure 1 shows measured chromatic dispersions for the two fibers. Considering a 4-nm source width, the bandwidth at zero dispersion can be obtained in the 1.5-μm wavelength region with the additional benefit of a larger core diameter than a step-index fiber.

In this paper we shall also present more recent data on fibers of this type. **(13 min)**

1. U. C. Paek, G. E. Peterson, and A. Carnevale, Bell Syst. Tech. J. **60**, 583 (1981).
2. U. C. Paek, G. E. Peterson, and A. Carnevale, Bell Syst. Tech. J. **60**, 1727 (1981).
3. M. A. Saifi, S. J. Jang, L. G. Cohen, and J. Stone, Opt. Lett. **7**, 43 (1982).

MF4 Ultrabroadband single-mode fibers

LEONARD G. COHEN, Bell Laboratories, Murray Hill, N.J. 07974; W. L. MAMMEL, Bell Laboratories, Crawford Hill Laboratory, Holmdel, N.J. 07733; S. J. JANG, Western Electric Engineering Research Center, P.O. Box 900, Princeton, N.J. 08540.

This paper will describe transmission properties of a new class of quadruple-clad (QC) lightguides which can provide low loss and low dispersion over the entire 1.3–1.6-μm spectral range.

Several previous publications have described how double-clad (DC) lightguide geometries[1] may be used to shape lightguide dispersion spectra to cancel material dispersion over a much broader wavelength range[2] [1.3–1.45 μm (Ref. 3) or 1.5–1.7 μm (Ref. 4)] than can conventional step-index single-clad (SC) single-mode fibers. Figure 1(a) shows the refractive-index profile structure that is typical of a DC lightguide with an inner cladding layer whose refractive index is substantially lower than that of the outer cladding (an index well). Ultrabroadband low-dispersion characteristics occur only if the fundamental mode cutoff wavelength λ_c is ~0.1 μm larger than the longest desired operational system wavelength. This requirement is necessary to make lightguide dispersion effects large enough to cancel material dispersion and to compensate for radiation leakage losses that are increased by bending the lightguide axis. Based on this criterion we have found that DC fibers cannot maintain low losses simultaneously with dispersion spectra zero crossings near 1.3 and 1.5 μm.

However, the fact that losses near 1.6 μm are due to leaky modes suggests that a practical way of reducing these losses may be to use a novel QC lightguide with two index wells [Fig. 1(b)], in which light leaking from the inner DC lightguide can be retrapped within the lightguide formed by the second, third, and fourth claddings.

The modified-chemical-vapor-deposition (MCVD) technique is being used to fabricate QC lightguide preforms. Preform-index profile data, as in Fig. 1, are analyzed[5] to specify the optimal fiber diameter for obtaining dispersion spectrum zero crossings near λ = 1.3 and λ = 1.55 μm simultaneously. Profile shapes are fabricated to yield fibers with core diameters of ~8 m and core-to-outer cladding-index differences of $\Delta_1 \sim 0.42\%$.

Figure 2(a) compares group-delay vs wavelength measurements, from 1-km lengths of QC fiber (——) DC fiber (– – –), and SC fiber (- - -). The curves were fitted to the data using a least-mean-square-fit procedure. Chromatic dispersion spectra in Fig. 2(b) were obtained by differentiating with respect to wavelength. Notice that the QC fiber dispersion is <2 psec/km-nm between the two zero crossings at λ = 1.3 and 1.6 μm. This low-dispersion spectral range is 2.5 times wider than the illustrated DC fiber spectra. Low-loss values can be maintained simultaneously with low dispersion. Specific loss values of the QC fiber described in Fig. 2 were 0.6 dB/km at λ = 1.3 μm and 0.4 dB/km at λ = 1.55 μm.

In this paper we survey the propagation characteristics of multiply clad fibers. In particular, we discuss the transmission properties and design considerations for the class of double-clad fibers and for the class of quadruple-clad fibers which have the potential for wavelength-division-multiplexing throughout the 1.3–1.55-μm wavelength range and have shown low dispersion and low loss over an ultrawide bandwidth range.

(invited paper, 13 min)

1. S. Kawakami and S. Nishida, IEEE J. Quantum Electron. **QE-10**, 879 (1974).
2. K. Okamoto, T. Edahiro, A. Kawana, and T. Miya, Electron. Lett. **15**, 729 (1979).
3. T. Miya, K. Okamoto, Y. Ohmori, and Y. Sasaki, IEEE J. Quantum Electron. **QE-17**, 858 (1981).
4. S. J. Jang, L. G. Cohen, W. L. Mammel, and M. S. Saifi, Bell Syst. Tech. J. **61**, 385 (1982).
5. W. L. Mammel and L. G. Cohen, Appl. Opt. **21**, 699 (1982).

MF5 Single-mode fiber with segmented core

V. A. BHAGAVATULA and P. E. BLASZYK, Corning Glass Works, Research & Development Division, Corning, N.Y. 14831.

Single-mode fibers with very low attenuation and dispersions in the 1.3- and 1.5-μm windows are essential for future long-distance telecommunications systems.

The main components of the total loss are the intrinsic fiber loss (Rayleigh scattering and absorption loss), splice loss, and microbend loss. To minimize the splice loss for a given lateral offset in the fiber cores, large spot sizes are needed. To minimize the losses due to bending and microbending perturbations, large propagation constants are required. For low total dispersion, fibers with steep waveguide dispersion are needed to compensate for the material dispersion. Summarizing, single-mode fiber designs with large spot sizes and propagation constants and steep waveguide dispersion characteristics are essential.

To date, single-mode fibers with step,[1] depressed clad (or *W*-type),[2] or triangular-index profiles[3] have been considered. These designs are expected to be only partially successful in meeting the requirements of low loss and low dispersion at 1.3 and 1.5 μm simultaneously. For example, step-index fibers with low loss or low dispersion at 1.3 μm are expected to have significant total dispersion at 1.5 μm. Low-dispersion depressed clad (or *W*-type) designs are expected to have large bending losses[2] or stringent tolerance requirements.[2] The results so far indicate the need for better optimization and also improved designs. To address some of these needs, a new design with segmented core (SEGCOR) is proposed.

An example of the index profile for the SEGCOR design is given in Fig. 1. This waveguide design consists of a core with an off-axis index depression Δ_d between radial locations indicated by *A*1 and *A*2. The core extends up to a radial location indicated by *A*. The propagation characteristics of the fiber can be modified by suitably controlling the parameters of the index depression. Examples of the variables that can be controlled are the radial position and depth and width of the index depression. The propagation characteristics of various SEGCOR designs have been estimated using a computer model[4] that solves the wave equation by direct numerical integration. An example of the normalized waveguide dispersion (Vd^2Vb/dV^2) is shown in Fig. 2. Here *V* and *b* represent the well-known normalized frequency and normalized propagation constants, respectively. In the same figure, the

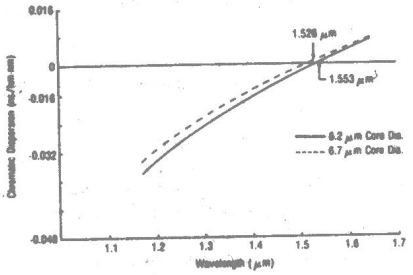

MF3 Fig. 1. Measured chromatic dispersions.

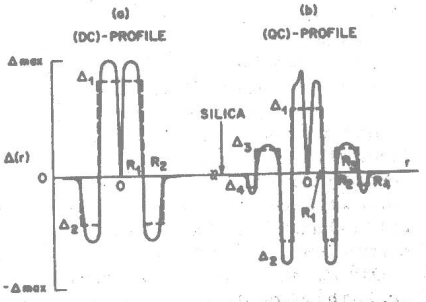

MF4 Fig. 1. Preform-index profile data: (a) refractive-index profile structure typical of a DC lightguide with an index well; (b) QC lightguide with two index wells.

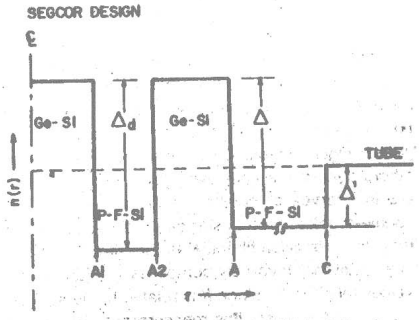

MF5 Fig. 1. Schematic diagram of the index profile for a SEGCOR design.

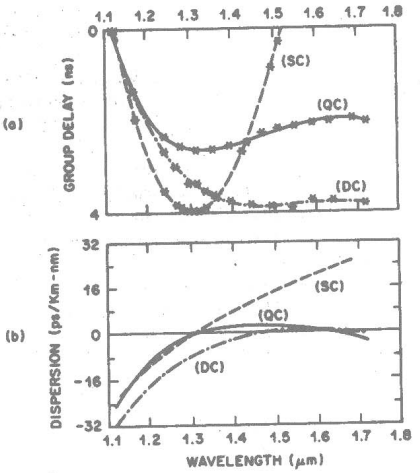

MF4 Fig. 2. Group-delay vs wavelength measurements.

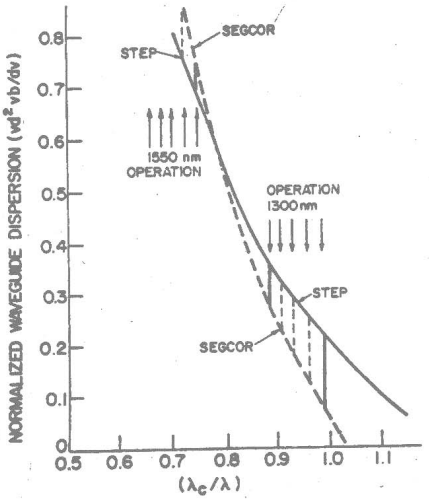

MF5 Fig. 2. Example of the computer calculations of the normalized waveguide dispersion for step-index and SEGCOR designs. The regions of operation for 1300 and 1550 nm are indicated.

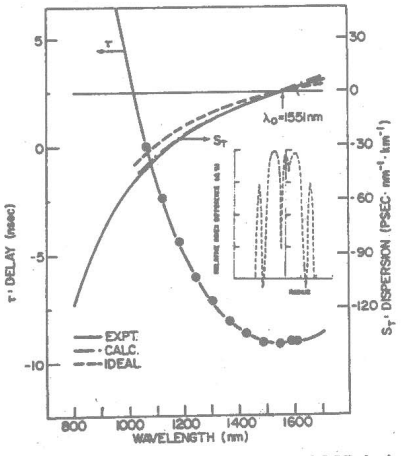

MF5 Fig. 3. Total dispersion of a SEGCOR design with zero dispersion wavelength at 1550 nm. The computer calculations for the actual fiber (- · -) and an ideal SEGCOR profile (- - -) are also plotted. Index profile of the SEGCOR fiber is shown in inset.

normalized waveguide dispersion for a step-index fiber is also shown. The SEGCOR design has a steeper variation of the waveguide dispersion compared with a step-index fiber. Also the waveguide dispersion of the SEGCOR design has much lower values at (λ_c/λ) values close to unity. Such a waveguide dispersion curve is expected to flatten the total dispersion curve leading to low total dispersion at both 1.3- and 1.5-μm windows. This improvement in waveguide dispersion for the SEGCOR design is achieved while maintaining comparable spot sizes to the earlier designs.

To experimentally verify the results of the computer modeling, fibers with SEGCOR design have been fabricated. Index profile of one such fiber along with its dispersion curve[5] with λ_0 at 1551 nm is shown in Fig. 3. Also shown in the figure are the calculated total dispersion and the dispersion for an ideal SEGCOR profile.

Details of the calculation for various SEGCOR designs along with additional experimental results will be presented. **(13 min)**

1. V. A. Bhagavatula, D. B. Keck, R. A. Westwig, and P. E. Blaszyk, in *Technical Digest, Topical Meeting on Optical Fiber Communication* (Optical Society of America, Washington, D.C., 1982), paper THCC4.
2. P. D. Lazay and A. D. Pearson, in *Technical Digest, Topical Meeting on Optical Fiber Communication* (Optical Society of America, Washington, D.C., 1982), paper THCC2; L. G. Cohen, W. L. Mammel, and S. Lumish, Opt. Lett. **7**, 183 (1982).
3. M. A. Saifi, S. J. Jang, L. G. Cohen, and J. Stone, Opt. Lett. **7**, 43 (1982).
4. V. A. Bhagavatula, Electron. Lett. **18**, 319 (1982).
5. W. F. Love, Corning Glass Works; private communication; in *Technical Digest, Sixth European Conference on Optical Communication*, U. York (1980).

MF6 Control of zero chromatic dispersion wavelength in fluorine-doped single-mode optical fibers

P. F. GLODIS, W. T. ANDERSON, and J. S. NOBLES, Bell Laboratories, 2000 Northeast Expressway, Norcross, Ga. 30071.

Germania-doped silica core single-mode fibers with depressed-index phosphorus–fluorine-doped silica cladding have been proposed for systems operating near 1.30 μm. The additional degree of freedom afforded by controlling the refractive index of the depressed cladding should allow a partial decoupling of core size and zero dispersion wavelength, extending the range of possible fiber designs.[1]

We have carried out an experimental study to determine the parameter range over which this advantage can be exploited to produce intrinsic low-loss high-bandwidth microbend-insensitive fiber. Approximately 50 fibers covering the range of interest in core size (6.5–9.0 μm) and Δ (0.30–0.52%) were included in the study.

The fibers were fabricated by the MCVD method in three groups, each with a different level of cladding depression. Several refractive-index profiles were obtained for each preform before fiber drawing to characterize each fiber length in terms of an equivalent step-index profile. An example is shown in Fig. 1. The spectral loss, cutoff wavelength, and zero dispersion wavelength were then measured for each fiber using standard techniques.

The dependence of the zero dispersion wavelength λ_0 was found to be well represented by the following form where d is the fiber core diameter and λ_c is the cutoff wavelength calculated from the equivalent step-index profile:

$$\lambda_0 = C_0 + \frac{C_1}{d}(1 - C_2\lambda_c).$$

The coefficients C were determined by least-squares fit to the zero dispersion wavelength measurements for each of the three cladding level groups.

The results are summarized in Fig. 2, which shows the range of core sizes over which a particular zero dispersion wavelength target can be realized if the measured fiber cutoff wavelength is constrained between the limits shown. The similarity of the results for the three cladding levels shows that the fiber dispersion is only weakly influenced by the cladding level once a minimum depression is obtained. The minimum zero dispersion wavelength which can be achieved is between 1.300 and 1.310 μm if the core diameter is held below 9 μm by microbending sensitivity considerations. If a higher zero dispersion wavelength (1.310–1.320 μm) can be tolerated, a relatively small core fiber (7.5–8.5 μm) can be used which should be highly resistant to microbending loss.

The abrupt long-wavelength loss increase typically seen in depressed cladding fibers[2] beyond a threshold wavelength was characterized in terms of a ratio R of the fiber loss at 1.55 μm (measured on a 7.5-cm radius reel) to the fiber loss at 1.30 μm. The open (shaded) areas in Fig. 2 represent designs with $R \leq 2.0$ ($R > 2.0$). If a low-loss high-dispersion window at 1.55 μm is required in addition to the primary low-dispersion window at 1.30 μm, the allowed design range is restricted, particularly in the deeper cladding cases. **(13 min)**

1. P. D. Lazay and A. D. Pearson, IEEE Trans Microwave Theory Tech. **MTT-30**, 350 (Apr. 1982).
2. P. D. Lazay, A. D. Pearson, and M. J. Saunders, in *Technical Digest, Topical Meeting on Optical Fiber Communication* (Optical Society of America, Washington, D.C., 1982), paper THCC2.

Monday **AFTERNOON**
28 February 1983 **MG**
BALLROOM H

2:00 PM Passive Optical Components: 1

P. Kaiser, Presider

MG1 Progress in the development of passive components

JOSEF STRAUS, Northern Telecom, Optical Systems Division, Ottawa, Ontario, Canada.

This paper will review the state of the art in the development of passive optical components, such as couplers, switches, wavelength division multiplexers, and optical isolators. The need for these components is evident from the increased number of systems installations, trials, and laboratory experiments which incorporate devices in their design.

Projections on future performance, cost, and commercial availability will also be discussed. **(Invited paper, 13 min)**

MG2 Optimizing cleaving tools by end-angle measurement

C. A. MILLAR and D. J. GOOCH, British Telecom Research Laboratories, Martlesham Heath, Ipswich, Suffolk IP5 7RE, U.K.

Flat and perpendicular fiber ends are essential for connectors and terminations to sources and detectors in measurement equipment. In monomode fiber splicing, properly cleaved ends reduce core distortion and the corresponding component of joint loss.[1] Although Gloge *et al.*,[2] extended the principles of glass fracture to optical fibers the choice of optimum cleaving conditions has yet to be verified experimentally. Using an end-angle measurement unit (EAMU) (a device based on diffraction of light by the cleaved end[3]), the angles of the endfaces are examined for different tool settings, fiber diameters, and glass compositions to find the optimum cleaving conditions.

Constant axial tension was applied to the fiber, which was clamped over a flat anvil. Ten end angles per tension setting were measured on EAMU and the mean of the sample calculated. The results for two fibers are shown in Fig. 1. Optimum tension settings exist for each fiber. An empirical relationship relating to optimum tension setting and the fiber composition and diameter has been found:

$$\frac{T_{opt}\sqrt{2r}}{\pi r^2} = K. \qquad (1)$$

This expression is an extension of the mirror formation formula, where the crack length to the mirror/mist zone at the optimum tension is equal to the fiber diameter. K is the mirror constant for the glass. Figure 2 plots T_{opt} for the fibers in Fig. 1 and others against the fiber diameter. Superimposed are the curves of constant K from Eq. (1). For double-crucible (composite glass) fibers $K = 4$ kg mm$^{-1.5}$. For silica fibers, $K = 7$ kg mm$^{-1.5}$, which is a result that favorably compares with published values for silica.[4] Since K is related to the surface energy of the glass, this measurement technique provides useful information about the fundamental strength properties of the fiber material.

Four anvil radii were studied: 20, 40, 60 mm, and ∞ (flat). The anvil material was polished steel in all cases, although rubber and plastic anvils performed in a similar manner. As shown in Fig. 3, there exists an optimum anvil radius between 60 mm and flat, but the difference between them is insignificant for standard 100–125-μm o.d. fiber. Larger diameters would require increasing amounts of anvil curvature to prevent hackle formation.

At T_{opt} Griffith[5] predicted a critical flaw size beyond which failure occurs:

$$L_c = \frac{2\pi E\gamma r^4}{T_{opt}^2}. \qquad (2)$$

The optimum condition would appear to be a flaw size which satisfies the Griffith equation and Eq. (1) simultaneously:

$$L_c[T_{opt}] = \frac{4E\gamma r}{\pi K^2}. \qquad (3)$$

Substituting the values of E, γ, and K for silica glass gives, for example, a theoretical optimum initiating flaw size of 3.4 μm for fiber 9128 at T_{opt}. Reproducible flaws of the correct size are induced by limiting the blade penetration into the glass with a micrometer stop and controlling the blade energy by a damped and loaded mechanism. The optimum blade conditions for fiber 9128 were: load = 10 gF; rate of travel = 10 mm/sec; and maximum penetration = 5 μm. For a constant blade energy (i.e., flaw size) the load and damping settings are predictably interchangeable. Blade material and edge geometry have a bearing on the blade energy/flaw size relationship and explain the deterioration in cleaving tool performance with blade wear.

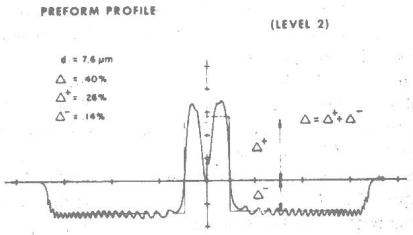

MF6 Fig. 1. Refractive-index profiles.

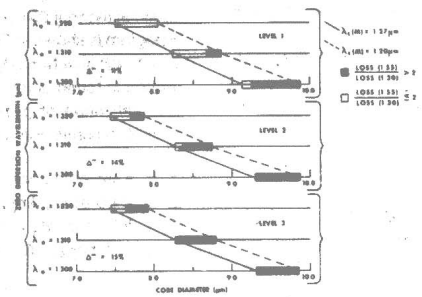

MF6 Fig. 2. Depressed cladding design possibilities.

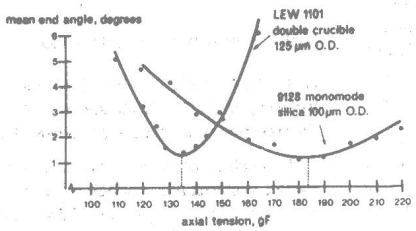

MG2 Fig. 1. Results for two fibers.

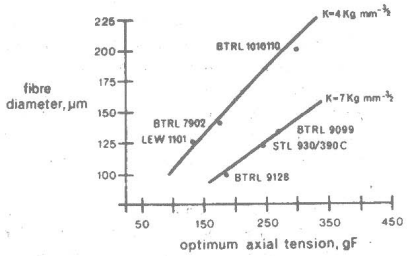

MG2 Fig. 2. T_{opt} plotted for fibers in Fig. 1.

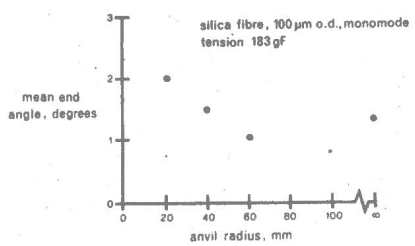

MG2 Fig. 3. Optimum anvil radius.

Skewness and torsion of the fiber during cleaving will be shown to have a deleterious effect on end preparation. Not all fibers are cleavable, suggesting an intrinsic component of fiber end angle due to the composition of the glass and/or the pulling and coating conditions.

Setting the optimum tension, blade energy, and anvil radius in a carefully designed cleaving tool resulted for fiber 9128 in a mean end angle of 0.54°, with a standard deviation of 0.32°. It is believed that the performance of the tool is optimum for most purposes, particularly in the important area of end preparation prior to splicing of monomode fibers. (13 min)

1. D. B. Payne and D. J. McCartney, at International Conference on Communications (Denver, 1980), paper 27.6.1.
2. D. Gloge *et al.*, Bell Syst. Tech. J. 52, 1579 (1973).
3. C. A. Millar, Opt. Quantum Electron. 13, 125 (1981).
4. R. W. Johnson and D. G. Holloway, Philos. Mag. 14, 731 (1951).
5. A. A. Griffith, Philos. Trans. R. Soc. London Ser. A 221, 163 (1921).

MG3 Realization of a low-loss splice for single-mode fibers in the field using an automatic arc-fusion splicing machine

TADATOSHI TANIFUJI and YASUYUKI KATO, NTT Ibaraki Electrical Communication Laboratory, Tokai, Ibaraki-ken 319-11, Japan; and SHIGEYUKI SEIKAI, NTT Research & Development Bureau, Musashino-shi, Tokyo 180, Japan.

To construct low-loss economical optical transmission lines using single-mode fiber cables, it is necessary to develop a splicing technique which can be used to join single-mode fibers with some core eccentricity and outer diameter discrepancy. Even for these fibers, low-loss arc-fusion splicing is expected with a precise core axis alignment technique in optimum fusion conditions. In this paper, we describe the optimum fusion conditions for low-loss splicing, construction of a splicing machine that realizes high-speed automatic axis alignment, and field trial results using the machine.

First, the optimum fusion conditions for single-mode fibers are considered. The surface tension effect at the fused point must be made as small as possible to avoid core metamorphosis and core axis misalignment for fibers with core eccentricity. The effect can be reduced by restricting the melting region, which is controlled by an electrode gap and a discharge duration. Figure 1 shows the dependence of splice loss on discharge duration T in splicing fibers with various core eccentricities. It is found that the splice loss and its fluctuation grow as T increases for fibers with large-core eccentricity of 4 μm. Other factors to affect the splice loss are prefusion time and fiber pressing stroke.[1] The optimum conditions for these factors have also been determined by experiments; they are summarized in Table I.

Next we describe a high-precision splicing machine with automatic axis alignment mechanisms. Figure 2 shows a block diagram of the splicing procedure using the machine. A LED and power meters are used to monitor the splice loss. Output optical power is received by OPM-2, and the signal is converted to serial data by MOD-2 and is sent to MOD-1 at the splicing point through interstitial pairs contained in the optical cable. At the splicing point, an automatic alignment controller (AAC) receives parallel data reconverted by MOD-1, and alignment mechanisms are driven by motors in x and y axes alternately so that the output optical power becomes maximum for each axis alignment. The sequence, one x alignment and one y alignment, is repeated about four times. Precise alignment mechanism without backlash is necessary to complete the sequence. Cantilever spring-type and leverage-type alignment mechanisms have been developed.[2] Alignment precision of 0.1 μm is attained for both types of mechanism. The time required for axis alignment depends on the initial misalignment. When butt joint loss is ~10 dB, it takes ~1 min for complete alignment. This time is satisfactorily short considering that at least 10 min are needed for manual alignment by unskilled operators.

The automatic splice machine was used in the field trial of a long-haul 400-Mb/sec transmission system using single-mode fiber cables designed at 1.3-μm[3] wavelength. The fibers were made by the MCVD and VAD methods; core diameter was ~10 μm, and fiber o.d. was 125 μm. Unit-type optical cables containing 6 or 12 fibers were installed into conduits along a 80-km long route. The splice loss histogram is shown in Fig. 3. An average splice loss of 0.11 dB is achieved, and the splice machine operation is found quite satisfactory. This promises the realization of practical low-loss single-mode optical transmission lines. (13 min)

1. Y. Kato *et al.*, Appl. Opt. 21, 1332 (1982).
2. Y. Kato *et al.*, Appl. Opt. 21, 1916 (1982).
3. Y. Ishida *et al.*, in *ICC'82 Conference Record, Vol. 1*, paper 5D1.1.

MG4 Low-loss field-installable biconic connectors for single-mode fibers

W. C. YOUNG and L. CURTIS, Bell Laboratories, Holmdel, N.J. 07733.

Molded biconic connectors are successfully being used in large quantities in the Bell System's multimode lightwave systems, with losses of the order of 0.5 dB routinely being achieved.[1] To obtain a similar performance with single-mode fibers, approximately an order of magnitude improved alignment tolerances are required. Typically single-mode fibers operating in the 1.3-μm wavelength region have core diameters between 8 and 10 μm. Therefore, to achieve losses of the order of 0.5 dB, the fiber cores have to be aligned to within 1.5 μm, and with an angular offset below 1°. As previously reported, this type of precision can be achieved with a taper-trimming technique, and losses of 0.28 dB (average) could readily be achieved with standard-toleranced fibers.[2] While this technique requires termination of the fibers before trimming, we describe in the following a field-installable connector plug that when used with existing multimode hardware, a more tightly toleranced biconic alignment sleeve that is selected from standard multimode sleeve fabrication, and precisely concentric fibers, also results in the required precision alignment and correspondingly low insertion losses (Fig. 1).

Using the same transfer-molding process previously employed for field-installable multimode connectors and laser plugs,[1] the single-mode connector plug is molded around a wire mandrel which creates a precision hole within the tapered plug. The wire diameter is chosen so that the resulting hole diameter is ~1 μm larger than the fiber to be terminated. To improve the precision of alignment between the hole and taper surface, the plug taper surface is subsequently ground concentric and coaxial with the central precision hole. The resulting hole-taper eccentricity for 22 plugs as measured with an automated test set[3] was 0.44 μm with a sigma of 0.22 μm, while the tilt angle between the hole and taper surface was immeasurably small (<0.1°). The plugs were installed onto 105-μm diam single-mode fibers with a 10-μm core and a cutoff wavelength of ~1.2 μm. The core–cladding eccentricity of these fibers was below 0.3 μm.

After assembly, the core-taper eccentricity of the single-mode plugs was 0.54 μm with a sigma of 0.21 μm (Fig. 2). The insertion loss was determined by randomly concatenating (nonoptimized) short lengths of connectorized single-mode fibers and recording the incremental loss as each connector was added. The mean loss of 22 such connections was 0.27 dB, with a sigma of 0.09 dB (Fig. 3). Fresnel reflection losses were avoided by designing for fiber endface contact. This was achieved by using the same connector endface finishing tool developed for the multimode connectors to create the proper taper length of the plug and provide the required endface flatness (<0.25 μm), all within a 1–2-min time period.

The widespread use of single-mode fibers in future lightwave communication systems will require low-loss connectors which can be installed both in the factory and in the field. A field-installable connector plug has been developed, which, when used with concentric-core fibers of known outer diameters, provides single-mode fiber interconnections with insertion losses of the order of 0.5 dB and below. The plugs can be used to terminate devices that are inherently fabricated with concentric-core fibers as well as to provide field terminations with some expected degradation in performance when the fibers have large core–cladding eccentricities and outer diameter variations. (13 min)

1. W. C. Young *et al.*, at *International Wire and Cable Symposium* (Cherry Hill, 1981).
2. W. C. Young, L. Curtis, and P. Kaiser, in *Technical Digest, Topical Meeting on Optical Fiber Communication* (Optical Society of America, Washington, D.C., 1982), postdeadline paper 5.
3. N. K. Cheung and N. M. Denkin, at *Symposium on Optical Fiber Measurement* (Boulder, Colo., 1980).

MG5 Pressure-tolerant fiber-optic feedthrough

C. A. VILLARRUEL, U.S. Naval Research Laboratory, Washington, D.C. 20375, and A. S. GREENBLATT, Sachs/Freeman Associates, Bowie, Md. 20715.

A number of fiber-optic communication and sensor systems are planned for use in underwater environments.[1] The successful implementation of these systems will require suitably designed pressure-tolerant fiber-optic componentry. To date, only cable designs for underwater applications have been reported.[2] Here we report on the design, implementation, and testing of a demountable multichannel low-loss multimode fiber pressure-tolerant feedthrough.

In this work, we use double-sided silicon V-grooved chips to align accurately twenty 100-μm core diam multimode fibers in a single planar layer. The Si V-grooved chips were fabricated much in the same manner as outlined by other authors.[3] Central to the fabrication of our device is the use of a two-part alignment disk with provisions for two Si chips and two precision alignment pins. Initially the Si chips are readily aligned to each other by placing several short fiber segments within the grooves; then, the Si chips are bonded to the top and bottom sides of a depression within the alignment disk. The Si chips serve to align the fibers only during the fabrication process and do not become part of the feedthrough. Thus they are reusable and assure interchangeability between feedthrough halves. Two precision pins are used to establish alignment between the two feedthrough halves. Later the same pins are used to reestablish their alignment

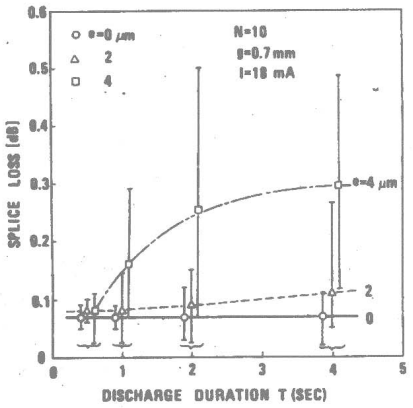

MG3 Fig. 1. Dependence of splice loss on electric discharge duration in splicing fibers with various core eccentricities. *N* denotes the number of data points.

MG3 Table I. Optimum Conditions for Single-mode Fusion Splicing

Electrode gap g(mm)	Prefusion time T_p(sec)	Electric discharge duration[a] T(sec)	Pressing stroke of fiber end face $S(\mu m)$	Discharge current I(mA)
0.7	0.2	1	20	18

[a] Including prefusion time.

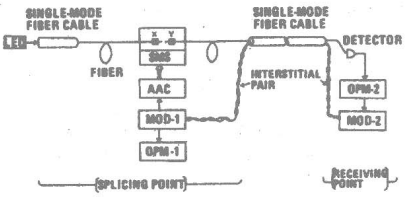

MG3 Fig. 2. Block diagram for automatic arc-fusion splice.

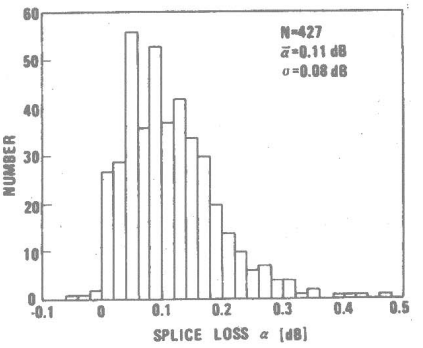

MG3 Fig. 3. Splice loss histogram in the field trial.

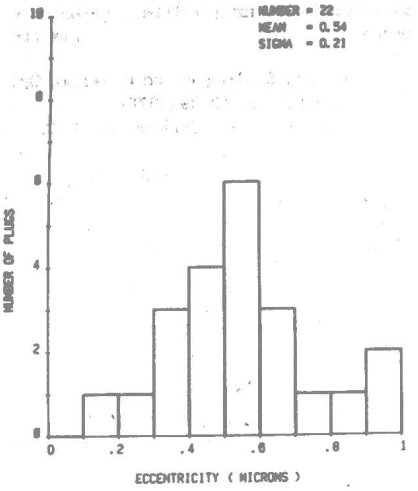

MG4 Fig. 2. Histogram. Transverse offset of the fiber core axis and the alignment taper axis.

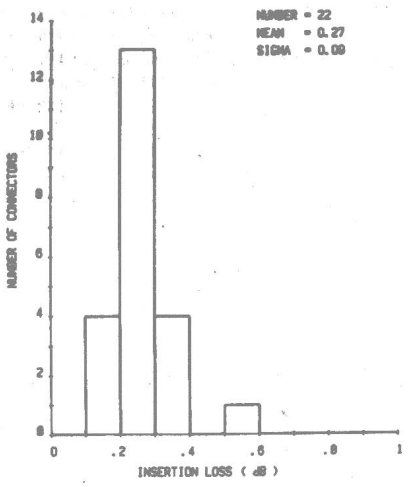

MG4 Fig. 3. Histogram. Insertion loss for 22 single-mode connections measured at 1.3 μm.

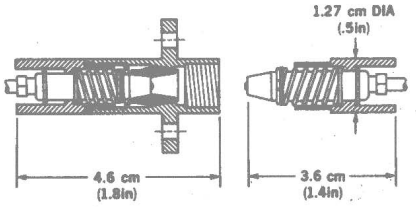

MG4 Fig. 1. Biconic connector for single-mode and multimode fibers.

MG5 Table I. Insertion Loss (dB)

FEEDTHROUGH NUMBER	MAXIMUM	MINIMUM	AVERAGE	ST. DEV.
1	2.0	.8	1.1	.4
2	1.5	.5	.7	.3
3	1.0	.2	.5	.2

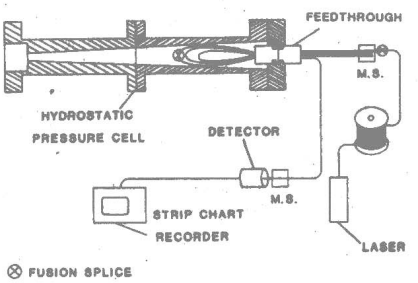

MG5 Fig. 1. Experimental arrangement used to measure insertion loss during pressure cycling.

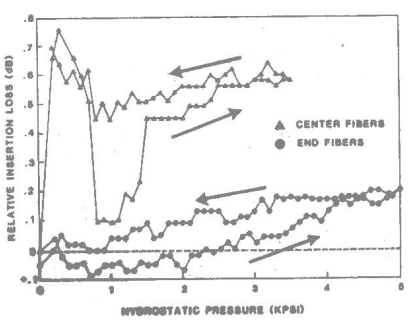

MG5 Fig. 2. Induced insertion loss due to pressure cycling. Insertion loss is referenced to atmospheric pressure loss. Arrows indicate pressurizing and depressurizing cycles.

during the mating cycle. Standard potting techniques are used to permanently encapsulate and fix the alignment of the fibers within the hexagonal spaces defined by the Si chips. Finally the two similarly processed halves, one from each side of the mold, are separated, and the fibers on the mating surfaces are mechanically polished to a suitable finish.

Three complete feedthroughs were fabricated and evaluated by measuring the insertion loss and cross talk before and during hydrostatic pressure cycling. Table I summarizes the measured insertion loss prior to pressure cycling. Interchangeability measurements showed an increase in loss of <0.5 dB from that of matched halves. In all cases, the measured cross talk was <30 dB. The experimental arrangement used to measure changes in the insertion loss during the hydrostatic pressure cycling is illustrated in Fig. 1. For this test, feedthrough 1 was modified by fusion splicing fibers to form continuous fiber loops. One loop was formed by splicing fibers located toward one end of the fiber array, while another loop was formed with fibers from the middle of the array. The measured sensitivity to hydrostatic pressure cycling up to 5 kpsi is illustrated in Fig. 2. Here, in all cases, the added loss is <1 dB, while the difference between the pressurizing and depressurizing cycles is <0.5 dB. Nonparallel polishing of the mating surfaces accounted for the higher insertion loss and greater pressure sensitivity of the loop formed with fibers from the middle of the array. Little or no permanent deformation of the fibers occurred during the pressure cycling. Further details of the feedthrough fabrication, hydrostatic, and shock pressure evaluation will be described.

(13 min)

1. C. D. Anderson, R. F. Gleason, P. T. Hutchinson, and P. K. Runge, IEEE Proc. **68**, 1299 (1980).
2. Z. K. Amand, IEEE J. Quantum Electron. **QE-18**, 697 (1982).
3. C. M. Schroeder, Bell Syst. Tech. J. **57**, 91 (1978).

MG6 Optical isolators for long-wavelength fiber-optic communication systems

R. C. BOOTH, D. COTTER, and E. A. D. WHITE, British Telecom Research Laboratories, Martlesham Heath, Ipswich, Suffolk IP5 7RE, U.K.

High-bit rate long-wavelength optical fiber communication systems are likely to require brpadband optical isolators capable of operating over the wavelength range containing both of the silica fiber loss minima, i.e., 1.3 and 1.55 μm. Present optical isolators are generally based on the magnetooptic Faraday effect and incorporate a suitable magnetooptic crystal, usually yttrium iron garnet $Y_3Fe_5O_{12}$, to rotate nonreciprocally by 45° the plane of polarization of the transmitted and reflected radiation.[1–3] Since the Faraday rotation is strongly wavelength dependent, these devices are narrow band and only produce useful optical isolation near the design wavelength.[1]

We have investigated the magnetooptic properties of a range of rare earth iron garnets in the 1.2–1.7-μm wavelength range. In particular we have determined that ytterbium iron garnet, $Yb_3Fe_5O_{12}$, possesses a wavelength-independent Faraday rotation of 5.7 ± 0.3° mm^{-1} for wavelengths greater than ~1.3 μm (Fig. 1). In this paper we show that devices made from this material provide, for the first time, high optical isolation throughout the important 1.3–1.7-μm wavelength range.

The optical isolator fabricated employed a $Yb_3Fe_5O_{12}$ crystal 7.89 mm thick as the active element (Fig. 2). The crystal was placed in a saturating axial magnetic field (~1200 Oe) between two polarizers with their respective polarization directions inclined at 45°. The extinction ratio of the isolator dB (ext) was measured as a function of wavelength (Fig. 3). (For the sake of experimental convenience these measurements were made by reversing the direction of the magnetic field rather than the direction of propagation, since these two configurations are known to be equivalent.[4]) It may be observed from Fig. 3 that for wavelengths longer than ~1.3 μm, the optical isolation is constant at 32 ± 3 dB. These wavelength-independent isolator characteristics are a substantial improvement over those obtained using optical isolators employing the conventional material $Yb_3Fe_5O_{12}$ where the extinction ratio falls by ~10 dB over a wavelength range as small as ~0.2 μm.

The extinction ratio of the isolator dB (ext) is related to the other figure of merit frequently reported for optical isolators, the optical isolation dB (isol), by the insertion loss of the device dB (ins), i.e., dB (ext) = dB (isol) − dB (ins). In this preliminary study the insertion loss of the device was typically ~7.5 dB of which the polarizers accounted for ~4.5 dB; reflections from the $Yb_3Fe_5O_{12}$ crystal, ~1.4 dB; and transmission loss through the crystal, ~1.5 dB. It is anticipated that with the use of improved polarizers, antireflection coatings, and some minor improvement in the optical quality of the $Yb_3Fe_5O_{12}$ crystals, the insertion loss could be reduced to 1–2 dB.

To summarize: a novel broadband magnetooptic $Yb_3Fe_5O_{12}$ isolator has been demonstrated, which, for the first time, provides wavelength-independent optical isolation throughout the 1.3–1.7-μm range currently of interest for optical fiber communication systems. **(13 min)**

1. H. Iwamura, S. Hayashi, and H. Iwaski, Opt. Quantum Electron. **10**, 39 (1978).
2. T. Matsumoto, Electron. Commun. Jpn. **62-C**, 113 (1979).
3. A. Shibukawa and M. Kobayashi, Electron. Lett. **14**, 816 (1978).
4. M. Torfeh, J. M. Desvignes, L. Courtois, and H. Le Gall, J. Appl. Phys. **49**, 1806 (1978).

MG7 High performance tuned fiber-coil isolators

GORDON W. DAY, DAVID N. PAYNE, A. J. BARLOW, and J. J. RAMSKOV-HANSEN, University of Southampton, Electronics Department, Southampton S09 5NH, U.K.

Faraday rotation in an optical fiber is normally quenched[1] by the presence of linear birefringence, either inherent to the fiber or induced by bending. However, this effect can be largely overcome by alternating the sense of the magnetic field along the length of the fiber in half-beat-length increments.[1–3] Since the beat length depends on wavelength, this leads to tuned devices providing an efficient interaction over a narrow range of wavelengths.

A coil of single-mode fiber in which the beat length is exactly equal to the circumference, placed in a magnetic field perpendicular to its axis, meets the condition for efficient interaction. Preliminary analysis and testing of such coils reported recently[3] have shown that their efficiency is half of that which would be obtained with a uniform magnetic field in the absence of linear birefringence. In this paper we demonstrate that isolators with very high isolation ratios and low insertion losses can thereby be produced.

The coils used in these experiments were constructed by winding inherently low-birefringence spun fiber[4] onto an accurately machined coil-former, coating the coil with adhesive, and removing the former. The birefringence of the coils then consists entirely of bend-induced birefringence and can be controlled to meet the tuning condition for a particular wavelength by choosing the coil diameter relative to the fiber diameter.[5] Fiber with a diameter of 180 μm and a 300-μm diam silicone jacket, wound on a 21.85-mm diam former, reproducibly gave coils that were within 0.1% of being correctly tuned at room temperature for a wavelength of 633 nm. The temperature coefficient of the bend birefringence was found to be 0.011%/°C (Fig. 1).

A 25-turn coil with these dimensions was sufficient to give >45° of Faraday rotation when placed in the field of a 0.3T permanent magnet. The loss of such coils (excluding coupling) was 0.3–0.4 dB. Since the field need not be uniform the rotation was adjusted to exactly 45° by moving the coil to the edge of the gap region where the field was slightly weaker. An isolator is then produced by placing polarizers with a relative orientation of 45° at the input and output so that light passing through the input polarizer and coil is also transmitted by the output polarizer. Light returning through the output polarizer, however, is rotated an additional 45° and is blocked by the input polarizer.

If the coil is detuned, that is, if at the wavelength of interest the beat length differs slightly from the circumference, light will be incompletely transmitted in the forward direction and incompletely blocked in the reverse direction. These effects can be quantitatively evaluated by numerical analysis of equations derived in Ref. 1. The principal parameter governing isolator performance is found to be the total (cumulative) birefringence error Δ_t in the coil rather than the fractional error.

The computed forward and reverse attenuations vs Δ_t are given by solid lines in Fig. 2. A reverse attenuation of >20 dB and a negligible forward attenuation are predicted for $\Delta_t < 0.1\pi$ rad. This value of Δ_t, which amounts to a fractional error of 0.2% for a 25-turn coil, is readily achieved with presently used fiber and winding techniques. The corresponding spectral width for 20 dB of isolation at 633 nm is 2.5 nm.

To verify the analysis we have measured the reverse attenuation of a group of coils, each with 25–27 turns but with different values of Δ_t. The results are given by the data points in Fig. 2. Departures from the predicted curve at values of Δ_t below 0.1π are believed to arise from slight bend- and stress-induced birefringence in the input and output leads. The best isolation ratio achieved to date is 44.5 dB.

We conclude that tuned fiber coil isolators with isolation ratios of >40 dB at their center wavelength can be routinely produced. These devices will have an isolation ratio of >20 dB over a spectral range of several nanometers or equivalently over a temperature range of ~35°C. **(13 min)**

1. W. J. Tabor, A. W. Anderson, and L. G. VanUitert, J. Appl. Phys. **41**, 3018 (1970).
2. R. H. Stolen and E. H. Turner, Appl. Opt. **19**, 842 (1980).
3. G. W. Day, D. N. Payne, A. J. Barlow, and J. J Ramskov-Hansen, Opt. Lett. **7**, 238 (1982).
4. A. J. Barlow, D. N. Payne, M. R. Hadley, and R. J. Mansfield, Electron. Lett. **17**, 725 (1981).
5. R. Ulrich, S. C. Rashleigh, and W. Eickhoff, Opt. Lett. **5**, 273 (1980).

MG8 Optical filters for wavelength division multiplexing

STEVEN BANDETTINI, Optical Coating Laboratory, Inc., 2789 Northpoint Parkway, Santa Rosa, Calif. 95401-7397.

Wavelength division multiplexing (WDM) provides a means for increasing optical communications system bandwidth with a minimum increase in the